Antibody incubation at 37°C improves fluorescent immunolabeling in free-floating thick tissue sections

Xia Xiao*, Ya-Ping Feng*, Bin Du, Han-Ru Sun, You-Quan Ding, and Jian-Guo Qi
Department of Histology, Embryology and Neurobiology, West China School of Preclinical and Forensic Medicine, Sichuan University, Chngdu, Sichuan, China

*X.X. and Y.-P.F. contributed equally to this work.

BioTechniques 62:115-122 (March 2017) doi 10.2144/000114524
Keywords: fluorescent immunolabeling; free-floating thick tissue section; whole-mount; three-dimensional quantification

Supplementary material for this article is available at www.BioTechniques.com/article/114524.

Fluorescent immunolabeling and imaging in free-floating thick (50–60 µm) tissue sections is relatively simple in practice and enables design-based non-biased stereology, or 3-D reconstruction and analysis. This method is widely used for 3-D in situ quantitative biology in many areas of biological research. However, the labeling quality and efficiency of standard protocols for fluorescent immunolabeling of these tissue sections are not always satisfactory. Here, we systematically evaluate the effects of raising the conventional antibody incubation temperatures (4°C or 21°C) to mammalian body temperature (37°C) in these protocols. Our modification significantly enhances the quality (labeling sensitivity, specificity, and homogeneity) and efficiency (antibody concentration and antibody incubation duration) of fluorescent immunolabeling of free-floating thick tissue sections.

Homeostasis, an essential feature of mammalian biological systems, operates at the level of the entire organism, within tissues or organ compartments, and within individual cells (1). Accurate quantification of molecular dynamics, cell number, cell shape, cell positioning and cell–cell interactions in tissues and organs is critical for quantitatively defining cellular and tissue homeostasis and screening for disease-specific stress or defense responses (1). This complicated task relies on high-quality 3-D in situ fluorescent immunolabeling and high-contrast fluorescent imaging of thick tissue sections or large tissue blocks (2–4), rather than traditional 2-D in situ chromogenic or fluorescent immunolabeling in thin tissue sections (3–10 mm), with its well-known biases (2–4) and low-contrast bright-field microscopic imaging.

Because it does not involve tissue sectioning, 3-D fluorescent immunolabeling and imaging of whole-mount large tissue blocks, including whole organs, is ideal for 3-D in situ quantitative biology (3–7). However, despite recent technical breakthroughs, methods for whole-mount 3-D fluorescent immunolabeling and imaging of large tissue blocks are complicated and require specialized facilities (3–7). In contrast, 3-D in situ quantitative biology, based on fluorescent immunolabeling and imaging of free-floating thick tissue sections (50–60 mm in thickness), is widely used in many areas of biological research. Free-floating thick tissue sections preserve 3-D structural information (2). This allows for design-based, non-biased stereology as well as 3-D reconstruction and analysis using standard microscopy, revealing molecular dynamics and allowing cellular profiling of mammalian tissues (2,3).

Standard protocols for fluorescent immunolabeling and imaging of free-floating thick tissue sections rely on tissue loosening using physical or chemical pretreatment (8–10), cell permeabilization using enhanced detergent treatment (8–11), enhanced antibody incubation (high concentrations or prolonged incubations for primary or secondary antibodies) at lower temperature (4°C) or at room temperature (RT) (21°C) (2,8–11), and optical sectioning microscopy such as confocal imaging (2,11). Previous studies showed that optical clearing-assisted, wide-field epifluorescent imaging and 3-D blind deconvolution allows high-quality 3-D visualization of thick tissue samples comparable to confocal imaging, making 3-D imaging of thick tissue sections simpler and more scalable (10,12). However, due to poor antibody penetration, standard protocols for fluorescent immunolabeling of free-floating thick tissue sections had an unsatisfactory labeling quality (low sensitivity for sparsely or moderately expressed proteins; faint or negative immunolabeling in the center of thick tissue sections and high non-specific binding) and an inadequate labeling efficiency (requiring high antibody concentrations and long antibody incubation times). These drawbacks render immunolabeling far from ideal for 3-D in situ quantitative biology applications (2,8,9,13).

It has been suggested that an increased antibody incubation temperature (such as 37°C, the mammalian body temperature), in contrast to the conventionally used incubation temperatures (4°C or 21°C), improves

METHOD SUMMARY

A standard fluorescent immunolabeling protocol is modified by increasing the antibody incubation temperature to mammalian body temperature (37°C), improving both the quality and efficiency of fluorescent immunolabeling of free-floating thick tissue sections.

fluorescent immunolabeling of thick tissue sections, possibly through enhancement of the penetration (14) or specific binding (15) of the antibody. Moreover, antibody incubation at 37°C has been extensively adopted in recently developed protocols for 3-D fluorescent immunolabeling of large tissue samples (such as iDISCO, ScaleS, Clarity, CUBIC, and SWITCH) (3–7). However, due to the lack of experimental validation, the rationale for antibody incubation at 37°C in fluorescent immunolabeling of large tissue samples, including thick tissue sections, remains controversial (8).

Here, we systematically validated the potential benefits of modifying the conventional antibody incubation temperature in standard protocols to 37°C for fluorescent immunolabeling of free-floating thick tissue sections. Compared with standard protocols, our modified protocol improves the quality and efficiency of fluorescent immunolabeling of free-floating thick tissue sections. These results suggest that antibody incubation at 37°C results in high-quality and efficient fluorescent immunolabeling for all types of large tissue samples, ranging from thick tissue sections to the whole organs. This improved 3-D fluorescent immunolabeling of large tissue samples will make 3-D in situ quantitative biology easier to implement in various areas of biological research.

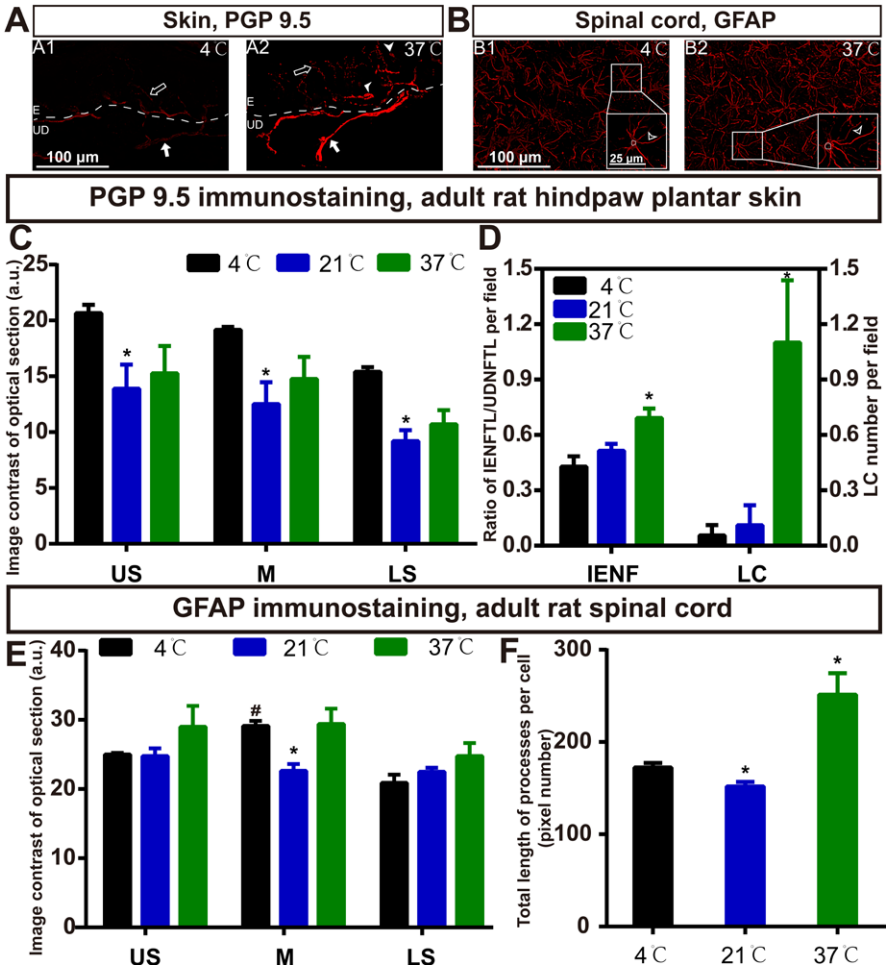

Figure 1. Effects of different antibody incubation temperatures on the quality and efficiency of fluorescent immunolabeling in free-floating thick (50-μm) tissue sections. Fluorescent PGP 9.5 (A,C,D) or GFAP (B,E,F) immunolabeling of adult rat hindpaw plantar skins or lumbar spinal cord with an antibody incubation temperature of 4°C, 21°C or 37°C were imaged with wide-field epifluorescence microscopes (3-D blind deconvolution and extended focus of depth) (A,B) and quantified for image contrast of optical sections (a.u.: arbitrary unit) (C,E); normalized length of intraepidermal nerve fiber (INEF) per field [ratio of INEF total length (INEFTL) to upper dermis nerve fiber (UDNF) total length (UDNFTL) per field; length unit: pixel number]; Langerhans cell (LC) number per field (D); and total length of processes per cell (unit: pixel number) (F). All experiments were independently repeated three times. Skin: E–epidermis; UD–upper dermis; dashed line–the dermo-epidermal junction; hollow arrow–INEF; solid arrow–UDNF; solid arrowhead–LC. Spinal cord: white box–100× snapshot of 20× region of interest (ROI); outline arrowhead–astrocyte process; closed circle,–astrocyte soma. *$P < 0.05$; compared with standard protocols with antibody incubation at 4°C. #$P < 0.05$; median (M) optical sections compared with upper surface (US) optical sections relative to microscopic objectives. Lower surface (LS) optical sections are not ideal controls of surface optical sections due to spherical aberration (Supplementary Figure S4).

Materials and methods

Animals

Twelve-week-old male adult Sprague-Dawley (SD) rats weighing 300–350 g at the beginning of the study were obtained from the Laboratory Animal Center of Sichuan University. The animals were housed with free access to standard chow and water in a room with an ambient temperature of 22 ± 1°C and a 12:12 h light/dark cycle. All animal manipulations were performed with the approval of the Animal Care and Ethics Committee of Sichuan University and in strict accordance with the National Institutes of Health (NIH) Guide for the Care and Use of Laboratory Animals (publication no. 85–23, revised 1985).

Fluorescent immunolabeling in free-floating thick tissue sections

After paraformaldehyde (PFA)-mediated transcardial perfusion fixation, the glabrous skins from both hindpaws and both sciatic nerves, as well as L4 lumbar spinal cord segments, were carefully removed. After immersion postfixation, sucrose cryoprotection, and embedding in optimum cutting temperature (OCT) medium (Sakura Finetek TissueTek; Torrance, CA), free-floating thick tissue sections (50 μm thick) were prepared on a cryostat (Leica CM3050S; Leica Instruments GmbH, Wetzlar, Germany). A detailed description of animal perfusion and histological processing is provided in the Supplementary Materials and Methods.

For intergroup comparison in individual experiments, three cohorts of animals with similar age and body weight (the numbers of animals per cohort depended on the numbers of experimental groups) were used for the preparation of free-floating thick tissue sections. For each cohort, three sections per animal were selected by a consistent program of systematic random sampling to achieve approximately the same anatomical locations for all of the sections used for intergroup comparison. Equal labeling among all experimental groups was insured by parallel processing from animal perfusion to tissue immunostaining. A detailed description of the fluorescent immunolabeling of free-floating thick tissue sections (including control settings) is provided in the Supplementary Materials and Methods and in Supplementary Figures S1 and S2.

In brief, after extensive washing with PBS-G (0.3 M glycine in 0.01 M PBS, pH 7.4) at RT, free-floating thick tissue sections were preconditioned for tissue loosening:

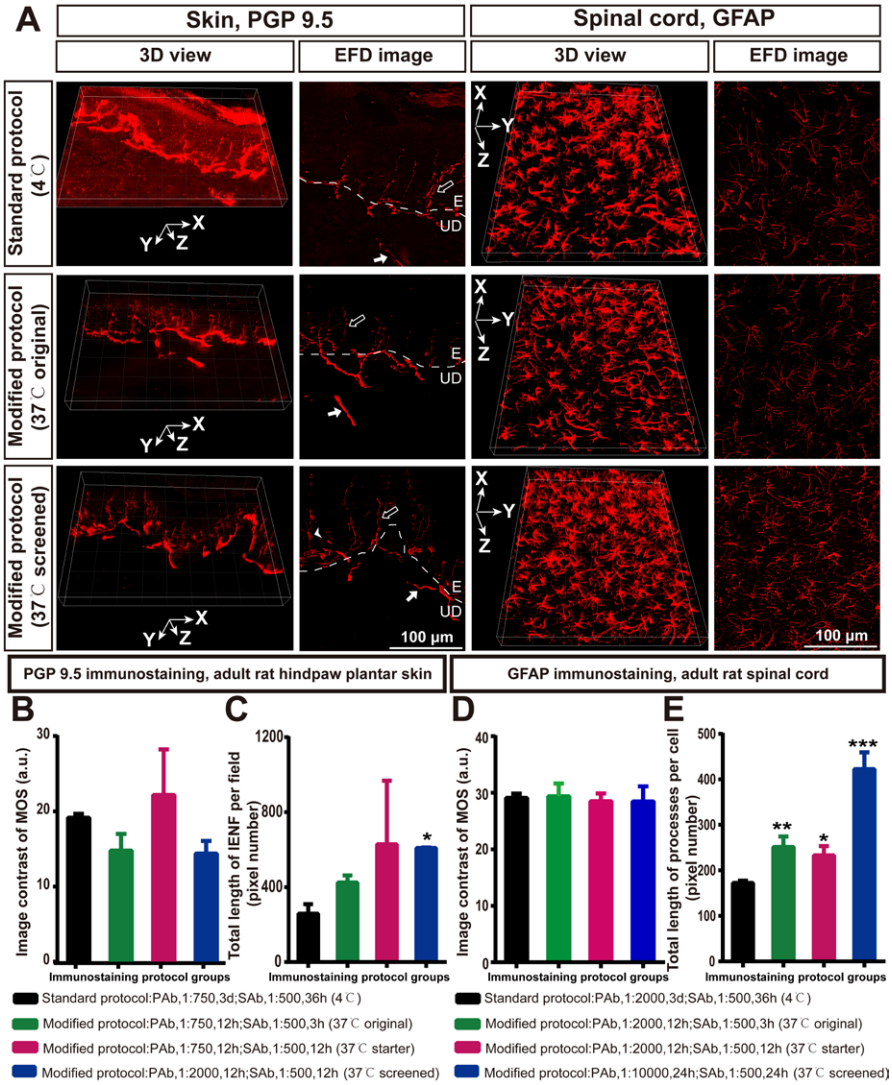

Figure 2. Improvement in quality and efficiency of fluorescent immunolabeling of free-floating thick (50 mm) tissue sections with an antibody incubation temperature of 37°C, based on orthogonal screening. (A) Representative post-deconvoluted 3-D view and extended focus of depth (EFD) images for fluorescent PGP 9.5 and GFAP immunolabeling of hindpaw plantar skins and lumbar spinal cords of adult rats, using standard protocol (antibody incubation at 4°C) and our modified protocols (antibody incubation at 37°C: original, orthogonal screening starter, orthogonal screened). The homogeneous immunolabeling (mean fluorescence intensities or image contrasts across the section depth) can be qualitatively visualized in 3-D view images. E–epidermis; UD–upper dermis; dashed line–the dermo-epidermal junction; outline arrow–intraepidermal nerve fiber (INEF); solid arrow–upper dermis nerve fiber (UDNF); solid arrowhead–Langerhans cell (LC). (B,C,D,E) Image contrasts (a.u.: arbitrary unit) of median optical sections (MOSs) for fluorescent PGP 9.5 (B) or GFAP (D) immunolabeling of hindpaw plantar skins or lumbar spinal cords of adult rats, total length of INEF per field (unit: pixel number) from fluorescent PGP 9.5 immunolabeling for adult rat hindpaw plantar skins (C), and total length of processes per cell (unit: pixel number) from fluorescent GFAP immunolabeling for adult rat lumbar spinal cords (E), using standard protocols (antibody incubation at 4°C) and our modified protocols (antibody incubation at 37°C: original, orthogonal screening starter, orthogonal screened). All experiments were independently repeated three times. $^{*}P < 0.05$, $^{**}P < 0.01$, and $^{***}P < 0.001$; compared with standard protocols. PAb: primary antibody; SAb: secondary antibody.

(*i*) skin: neat DMSO for 15 min to loosen collagen structures in the upper dermis (UD) and dense cellular networks in the epidermis (10); (*ii*) spinal cord: antigen retrieval with sodium citrate solution (0.01 M sodium citrate, 0.05% Tween-20, pH 6.0) at 80°C for 45 min to improve antigenic reactivity and antibody penetration (9,11); and (*iii*) sciatic nerve: thermally-assisted delipidation with 0.2 M sodium dodecyl sulfate (SDS) (in PBS, pH 9.0) at 37°C for 3 h (7). After extensive washing with PBST (0.2% Tween-20 in 0.01 M PBS, pH 7.4) at RT, thick tissue sections were then permeabilized with PBS-Tx (0.3% Triton X-100 in 0.01 M PBS, pH 7.4): 4 × 15 min for skin and spinal cords, and 6 × 15 min for sciatic nerves.

After extensive washing with PBST, sections were inactivated with PBST-G (0.3 M glycine in PBST, pH 7.4) for 15 min at RT, and blocked with the blocking buffer [0% normal goat serum (NGS) and 1% BSA in 0.01 M PBS, pH 7.4, containing 0.05% Tween-20 and 0.01% sodium azide] for 2 h at RT. Then, sections were incubated with primary antibodies diluted in blocking buffer with gentle agitation for 3 days at 4°C, 12 h at RT or 3–72 h at 37°C (dilution ratios and incubation durations indicated in Supplementary Figure S2). The following primary antibodies were used for skin or sciatic nerve sections: rabbit polyclonal anti-PGP 9.5 (14730–1-AP; Proteintech, Wuhan, Hubei, China), mouse monoclonal anti-NF200 (N0124, clone N52; Sigma-Aldrich, St. Louis, MO), rabbit polyclonal anti-peripherin (17399–1-AP; Proteintech), and goat polyclonal anti-CGRP (36001; Abcam, Cambridge, UK). For spinal cord sections, the following primary antibodies were used: mouse monoclonal anti-GFAP (60190–1-Ig; Proteintech), mouse monoclonal anti-NeuN (104224; Abcam), rabbit polyclonal anti-Iba1 (10904–1-AP; Proteintech), and rabbit polyclonal anti-Olig2 (13999–1-AP; Proteintech). After washing 6 × 15 min each in PBST at RT, the sections were incubated with highly cross-adsorbed goat anti-rabbit or mouse IgG secondary antibodies conjugated to Alexa Fluor 594 (ab150080 or 150116; Abcam) or highly cross-adsorbed donkey anti-goat IgG secondary antibodies conjugated to Cy3 (ab6949; Abcam) with gentle agitation for 36 h at 4°C, 3 h at RT, or 3–36 h at 37°C (dilution ratios and incubation durations indicated in Supplementary Figure S2).

After extensive washing with PBST, tissue sections were processed for optical clearing with gradient glycerol solutions (diluted in 0.01 M PBS, pH 8.0, 2.5% DABCO, 0.05% Tween-20) as previously described (10,16). Sections were mounted on poly-L-lysine (PLL)-coated slides with the anti-fade mounting medium (2.5% DABCO, 0.05% Tween-20 in 90% glycerol diluted with 0.01 M PBS, pH 8.0) overnight at 4°C. Optionally, before optical clearing, all the skin sections were re-fixed with histological fixatives (4% PFA in 0.1 M PB, pH 7.4) for 1 h at 4°C, inactivated with PBSG for 1 h at 4°C, and washed with PBST 3 × 15 min at RT.

Image acquisition and processing

For imaging convenience and scalability, we utilized optical clearing-assisted, wide-field epifluorescent imaging and 3-D blind deconvolution, which were shown in previous studies by our group and others to enable high-contrast 3-D visualization of thick tissue samples comparable to confocal imaging

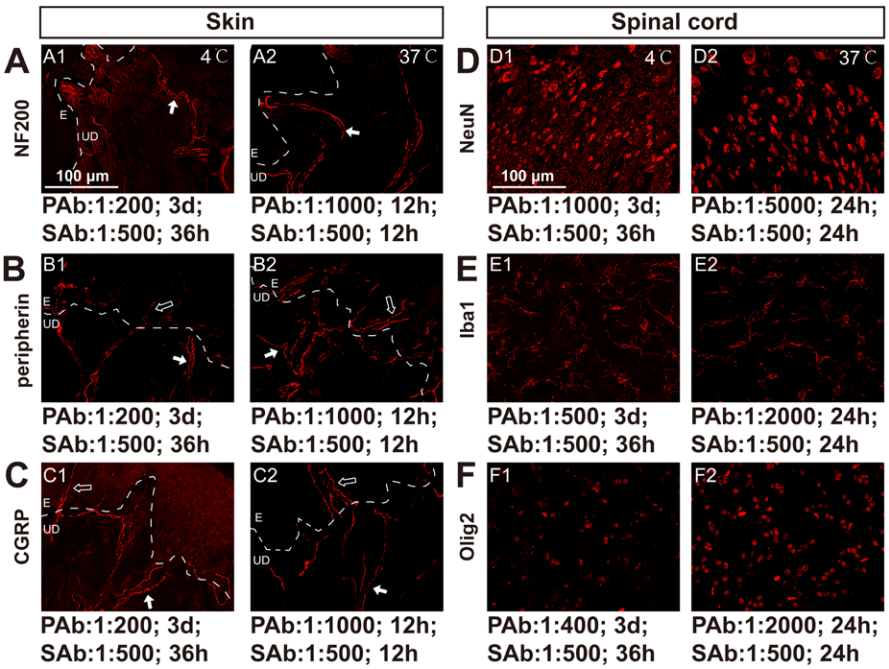

Figure 3. The benefits, independent of antibody or antigen characteristics, of antibody incubation at 37°C for fluorescent immunolabeling of free-floating thick (50 µm) tissue sections. (A,B,C) Representative post-deconvoluted, extended focus of depth (EFD) images for fluorescent immunolabeling of thick tissue sections from adult rat hindpaw plantar skins with antibodies against NF200 (A), peripherin (B), and CGRP (C), using a standard protocol [antibody incubation at 4°C] and our modified protocol [antibody incubation at 37°C, based on orthogonal screening of primary antibody incubation parameters (Supplementary Figure S2C)]. E–epidermis; UD–upper dermis; dashed line–the dermo-epidermal junction; outline arrow–intraepidermal nerve fiber (INEF); solid arrow–upper dermis nerve fiber (UDNF). (D,E,F) Representative post-deconvoluted, EFD images for fluorescent immunolabeling of thick tissue sections from adult rat lumbar spinal cords with antibodies against NeuN (D), Iba1 (E), and Olig2 (F), using a standard protocol (antibody incubation at 4°C) and our modified protocol [antibody incubation at 37°C, based on orthogonal screening of primary antibody incubation parameters (Supplementary Figure S2D)]. All experiments were independently repeated three times. PAb: primary antibody; SAb: secondary antibody.

(10,12). All of the fluorescently immunolabeled free-floating thick tissue sections were imaged using a fully motorized, Olympus IX-83 widefield (WF) epifluorescence microscope with a DP80 CCD camera under the monochromatic mode controlled by Olympus cellSens Dimension software (Olympus; Tokyo, Japan) (10). For PGP 9.5 immunolabeling of sciatic nerve thick sections, Z-stack images of the same sections were further captured on an Olympus FV1000 confocal microscope for better evaluation of antibody diffusion in sciatic nerve thick sections. Details for Z-stack image acquisition of WF or confocal epifluorescence optical sections across the section depth are provided in the Supplementary Materials and Methods.

All of the WF original Z-stack images were quantified using Fiji software (NIH, Bethesda, Maryland) for image contrasts (17) and mean intensities (8) of optical sections along the imaging depth normalized to the original tissue section thickness (Supplementary Figures S3 and S4). All of the corresponding extended focus of depth (EFD) images by the extended focus tool in the cellSens Dimension software were quantified using Fiji software for mean pixel intensities (MPIs) of the foreground (object) and the background (Supplementary Figure S3). For PGP 9.5 immunolabeling of skin thick sections or GFAP immunolabeling of spinal cord thick sections, those EFD images were further quantified using Fiji software for the signals of the detailed objects in tissue sections (Supplementary Materials and Methods, Supplementary Figure S3). Those quantitative data were used for the evaluation of the quality (sensitivity, specificity, and homogeneity) of fluorescent immunolabeling in free-floating thick tissue sections.

Representative WF original image stacks were selected for 3-D blind deconvolution by AutoQuant X3 (Media Cybernetics; Rockville, MD). The WF deconvoluted image stacks were used to create EFD images with Image Pro Plus7.0 software (Media Cybernetics), individual images for upper surface (US), median (M) and lower surface (LS) optical sections with Fiji software, and 3-D view images with Imaris 7.4.2 (64-bit version) (Bitplane; Belfast, UK). All of those images were exported in the 8-bit TIFF format for the assembly of figures for this publication with Adobe Illustrator CC 2014 (Adobe, San Jose, CA).

Statistical analysis

All of the quantitative data for the quality of fluorescent immunolabeling in free-floating thick tissue sections are presented as mean ± SEM (due to their normal distribution pattern) and statistically analyzed with IBM SPSS Statistics 22.0 (IBM; Armonk, NY). Details of statistical comparisons for individual experiments are provided in the Supplementary Materials and Methods. For all of the data analyses, a P value <0.05 was considered statistically significant. All of the statistical graphs were plotted using GraphPad Prism 6.01 (GraphPad Software, Inc.; Northampton, MA) and assembled into the figures of this publication with Adobe Illustrator CC 2014.

Results and discussion

Thick skin sections of plantar surfaces from adult rat hindpaws were initially used to validate the benefits of optimal antibody incubation temperature for fluorescent immunolabeling in free-floating thick tissue sections. The conventional antibody incubation temperature (4°C or 21°C) in standard protocols was modified to 37°C, and we used a primary antibody against PGP 9.5 (an intra-axonal cytosolic protein) as an example. The very high densities of extracellular matrix (ECM) components in the dermis and cellular components in the

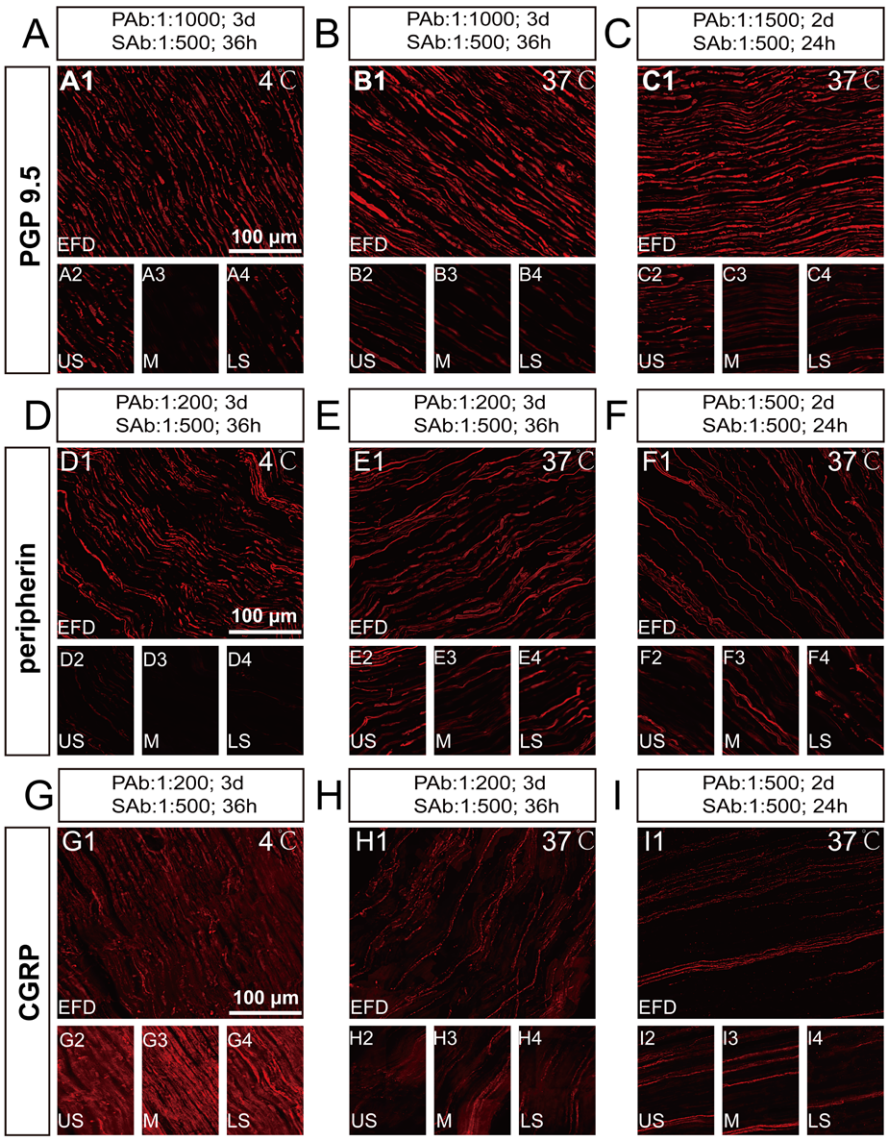

Figure 4. Benefits of antibody incubation at 37°C for fluorescent immunolabeling of free-floating thick (50 mm) sections of adult rat sciatic nerves. Representative post-deconvoluted, extended focus of depth (EFD) images and individual images for upper surface (US), median (M), and lower surface (LS) optical sections for fluorescent immunolabeling of thick tissue sections from adult rat sciatic nerves using antibodies against PGP 9.5 (A,B,C), peripherin (D,E,F), and CGRP (G,H,I), using a standard protocol (antibody incubation at 4°C) (A,D,G), our initial modified protocol (antibody incubation at 37°C with the same primary antibody incubation parameters as antibody incubation at 4°C) (B,E,H), and our final modified protocol [antibody incubation at 37°C, based on orthogonal screening of primary antibody incubation parameters (Supplementary Figure S2E)] (C,F,I). All experiments were independently repeated three times. PAb: primary antibody; SAb: secondary antibody.

epidermis pose great challenges for specific binding and penetration of antibodies (4,10,18). A previous study showed that tissue loosening by DMSO pretreatment significantly improves fluorescent immunolabeling of free-floating thick skin sections (10). In the present study, our results show that, compared with antibody incubation at 4°C or 21°C, antibody incubation at 37°C substantially improved the fluorescent visualization of upper dermis nerve fibers (UDNFs) (data not shown), intraepidermal nerve fibers (IENFs), and Langerhans cells (LCs), with contrasts or intensities comparable to and even higher than those for antibody incubation at conventional temperatures (Figure 1, A, C, and D; Supplementary Figures S5 and S6). Moreover, antibody incubation at 37°C drastically shortened the incubation durations necessary for achieving complete and even antibody penetration along the axial depth (Figure 1C; Supplementary Figures S5 and S6), and reduced patchy non-specific antibody binding and uniform background signal (especially at the surfaces of thick skin sections) (Supplementary Figure S5).

We next employed GFAP (astrocyte marker, cytoskeleton protein) immunolabeling in free-floating thick sections of adult rat spinal cords (7) to characterize the potential benefits of antibody incubation at 37°C. It has been suggested that specific and non-specific entrapment at the surfaces of thick tissue sections of antibodies against highly abundant and widely expressed proteins (such as GFAP in adult spinal cord) is the main contributor to the difficulty of antibody penetration into the central areas (3,7,19). We found that antibody incubation at 37°C significantly increased antibody penetration along the depth of the section, enhanced specific immunolabeling to make even detailed objects (such as astrocyte processes) robustly visible, and reduced the uniform background signal (Figure 1, B, E, and F; Supplementary Figure S7). Therefore, antibody incubation at 37°C for fluorescent immunolabeling of free-floating thick tissue sections could simultaneously reduce antibody incubation durations for homogeneous immunolabeling along the section depth and improve immunolabeling quality.

To identify any additional benefits of antibody incubation at 37°C during fluorescent immunolabeling of free-floating thick tissue sections, we screened for optimal incubation durations and optimal concentrations for primary antibodies and secondary antibodies at 37°C by an orthogonal experimental design (Supplementary Figure S2, A and B). Incubation durations for secondary antibodies (1:500, 37°C) during parameter screening for primary antibodies were set to be the same as those for primary antibodies to exclude the negative impact of insufficient secondary antibody incubation on the quality of primary antibody immunolabeling (Supplementary Figure S2A) (3,20). For fluorescent PGP 9.5 immunolabeling in thick skin sections, in contrast to antibody incubation at 4°C (primary antibody: 3 days, 1:750; secondary antibody: 36 h, 1:500), primary antibody incubation parameters (12 h, 1:2000) and secondary antibody incubation parameters (12 h, 1:500) at 37°C stably achieved the highest sensitivity and specificity of homogeneous immunolabeling along the section depth, manifested as relatively robust visualization of the detailed objects (such as IENFs and LCs) and substantial reductions of the patchy signals for non-specific antibody binding or uniform background signals (Figure 2, A, B, and C; Supplementary Figures S8 and S9). Similarly, for fluorescent GFAP immunolabeling in thick spinal cord sections, in contrast to antibody incubation at 4°C (primary antibody: 3 days,

1:2000; secondary antibody: 36 h, 1:500), primary antibody incubation parameters (24 h, 1:10000) and secondary antibody incubation parameters (24 h, 1:500) at 37°C were found to mostly improve the quality of homogeneous immunolabeling along the section depth (Figure 2, A, D, and E; Supplementary Figures S10 and S11). Thus, antibody incubation at 37°C has the ability to improve the quality (sensitivity, specificity, and homogeneity) and efficiency (antibody incubation duration and concentration) of fluorescent immunolabeling of free-floating thick tissue sections.

To further validate the ability of antibody incubation at 37°C to improve the quality and efficiency of fluorescent immunolabeling in free-floating thick tissue sections, we employed more primary antibodies from different animal species, either monoclonal or polyclonal, targeting antigens of different subcellular localizations (membrane-localized, cytoskeletal, cytosolic and nucleus, neuronal, and non-neuronal antigens). Our orthogonal screening results showed that, in contrast to antibody incubation at 4°C, antibody incubation at 37°C improved the quality and efficiency of fluorescent immunolabeling of NF200, peripherin, and CGRP in thick skin sections (Figure 3, A, B, and C; Supplementary Figure S12, A, B, and C) or NeuN, Iba1, and Olig2 in thick spinal cord sections (Figure 3, D, E, and F; Supplementary Figure S12, D, E, and F).

Adult rat peripheral nerves should be one of the most challenging structures for diffusion-based penetration of primary antibodies against axonal proteins since there are very dense cellular and ECM networks in their endoneurium, a large amount of sphingolipids around myelinated axons, and highly abundant axonal proteins. This notion was supported by our results, showing that prolonged antibody incubation at 4°C, even after thermally-assisted SDS delipidation, still resulted in faint or negative immunolabeling against PGP 9.5, peripherin, and CGRP in the center of thick sciatic nerve sections (Figure 4, A, D, and G; Supplementary Figure S13A). In contrast, antibody incubation at 37°C with the same parameters for antibody incubation concentrations and durations showed significant improvement of antibody penetration and immunolabeling along the section depth (Figure 4, B, E, and H; Supplementary Figure S13). Moreover, our orthogonal screening results showed that antibody incubation at 37°C improved the quality and efficiency of fluorescent immunolabeling in thick nerve sections (Figure 4, C, F, and I).

Compared with standard protocols for immunofluorescent staining of free-floating thick tissue sections using conventional antibody incubation temperatures (4°C or 21°C), our modified protocol with antibody incubation at 37°C demonstrated improved quality (sensitivity, specificity, and homogeneity) and efficiency (antibody incubation duration and concentration) of fluorescent immunolabeling, independent of antibody, antigen, and tissue characteristics. One possible mechanism for this effect could be that the higher mobility of antibody during incubation at 37°C promotes antibody penetration across the section depth (14), and enhancement of interactions between flexible antigen epitopes and highly mobile antibodies at 37°C improves immunolabeling sensitivity (15) and specificity. However, our preliminary results (data not shown) suggest that the enhancement of antibody penetration into thick tissue sections by antibody incubation at 37°C were dependent on intense chemical or physical pretreatment

to loosen tissue structures. This could explain the controversial results of previous studies (8,14,15) in which antibody incubation at 37°C without tissue loosening were shown to have little or no ability to increase antibody diffusion.

Most antibodies used in biological research are produced in mammalian biological systems with physiological body temperatures of ~37°C. Consequently, these antibodies should be evolved so that 37°C is the optimal temperature for their specific and efficient interaction with the corresponding antigens residing deep within tissues and organs. Therefore, it is likely that the improvement in fluorescent immunolabeling of free-floating thick tissue sections with antibody incubation at 37°C should be generalizable. This suggests antibody incubation at 37°C is necessary for the efficient 3-D fluorescent immunolabeling of other large tissue samples, such as whole organs.

Author contributions

X.X. and Y-P.F. conducted all of the experiments and analyzed the data. B.D. and H.-R.S. analyzed the data. Y.-Q.D. and J.-G.Q. designed the study, analyzed the data and wrote the manuscript. J.-G.Q. supervised the project.

Acknowledgments

This work reported was supported by grants from the National Science Foundation of China (31571240), the Sichuan Province Science and Technology Support Program (2013SZ0069), and the educational reform program (Year 2016) for experimental courses of Sichuan University (501164010) to J.-G.Q.

Competing interests

The authors declare no competing interests.

References

1. **Chovatiya, R. and R. Medzhitov.** 2014. Stress, inflammation, and defense of homeostasis. Mol. Cell *54*:281-288.
2. **Schmitz, C., B.S. Eastwood, S.J. Tappan, J.R. Glaser, D.A. Peterson, and P.R. Hof.** 2014. Current automated 3D cell detection methods are not a suitable replacement for manual stereologic cell counting. Front. Neuroanat. *8*:27. 10.3389/fnana.2014.00027.
3. **Renier, N., Z. Wu, D.J. Simon, J. Yang, P. Ariel, and M. Tessier-Lavigne.** 2014. iDros. Inf. Serv.CO: a simple, rapid method to immunolabel large tissue samples for volume imaging. Cell *159*:896-910.
4. **Hama, H., H. Hioki, K. Namiki, T. Hoshida, H. Kurokawa, F. Ishidate, T. Kaneko, T. Akagi, et al.** 2015. ScaleS: an optical clearing palette for biological imaging. Nat. Neurosci. *18*:1518-1529.
5. **Chung, K., J. Wallace, S.Y. Kim, S. Kalyanasundaram, A.S. Andalman, T.J. Davidson, J.J. Mirzabekov, K.A. Zalocusky, et al.** 2013. Structural and molecular interrogation of intact biological systems. Nature *497*:332-337.
6. **Susaki, E.A., K. Tainaka, D. Perrin, F. Kishino, T. Tawara, T.M. Watanabe, C. Yokoyama, H. Onoe, et al.** 2014. Whole-brain imaging with single-cell resolution using chemical cocktails and computational analysis. Cell *157*:726-739.
7. **Murray, E., J.H. Cho, D. Goodwin, T. Ku, J. Swaney, S.Y. Kim, H. Choi, Y.G. Park, et al.** 2015. Simple, scalable proteomic imaging for high-dimensional profiling of intact systems. Cell *163*:1500-1514.
8. **Melvin, N.R. and R.J. Sutherland.** 2010. Quantitative caveats of standard immunohistochemical procedures: implications for optical disector–based designs. J. Histochem. Cytochem. *58*:577-584.
9. **Hou, J., J. Riise, and B. Pakkenberg.** 2012. Application of immunohistochemistry in stereology for quantitative assessment of neural cell populations illustrated in the Göttingen minipig. PLoS One *7*:e43556. 10.1371/journal.pone.0043556.
10. **Ren, H.Y., Y.Q. Ding, X. Xiao, W.Z. Xie, Y.P. Feng, X.Y. Li, and J.G. Qi.** 2016. Behavioral characterization of neuropathic pain on the glabrous skin areas reinnervated solely by axotomy-regenerative axons after adult rat sciatic nerve crush. Neuroreport *27*:404-414.
11. **Beggs, S. and M.W. Salter.** 2007. Stereological and somatotopic analysis of the spinal microglial response to peripheral nerve injury. Brain Behav. Immun. *21*:624-633.
12. Epp, J.R., Y. Niibori, H.L. Liz Hsiang, V. Mercaldo, K. Deisseroth, S.A. Josselyn, and P.W. Frankland. 2015. Optimization of CLARITY for clearing whole-Brain and other intact organs. eNeuro. 2. pii: ENEURO.0022-15.2015. doi: 10.1523/ENEURO.0022-15.2015.
13. **Fouquet, C., J.F. Gilles, N. Heck, M. Dos Santos, R. Schwartzmann, V. Cannaya, M.P. Morel, R.S. Davidson, et al.** 2015. Improving axial resolution in confocal microscopy with new high refractive index mounting media. PLoS One *10*:e0121096. 10.1371/journal.pone.0121096.
14. **Gleave, J.A., J.P. Lerch, R.M. Henkelman, and B.J. Nieman.** 2013. A method for 3D immunostaining and optical imaging of the mouse brain demonstrated in neural progenitor cells. PLoS One *8*:e72039. 10.1371/journal.pone.0072039.
15. **Wouterlood, F.G., M.E. Boon, and L.P. Kok.** 1990. Immunocytochemistry on free-floating sections of rat brain using microwave irradiation during the incubation in the primary antiserum: light and electron microscopy. J. Neurosci. Methods *35*:133-145.
16. **Selever, J., J.Q. Kong, and B.R. Arenkiel.** 2011. A rapid approach to high-resolution fluorescence imaging in semi-thick brain slices. J. Vis. Exp. *53*:2807. 10.3791/2807.
17. **Costantini, I., J.P. Ghobril, A.P. Di Giovanna, A.L. Allegra Mascaro, L. Silvestri, M.C. Müllenbroich, L. Onofri, V. Conti, et al.** 2015. A versatile clearing agent for multi-modal brain imaging. Sci. Rep. *5*:9808. 10.1038/srep09808.
18. **Lee, E., J. Choi, Y. Jo, J.Y. Kim, Y.J. Jang, H.M. Lee, S.Y. Kim, H.J. Lee, et al.** 2016. ACT-PRESTO: rapid and consistent tissue clearing and labelling method for 3-dimensional (3D) imaging. Sci. Rep. *6*:18631. 10.1038/srep18631.
19. **Kim, S.Y., J.H. Cho, E. Murray, N. Bakh, H. Choi, K. Ohn, L. Ruelas, A. Hubbert, et al.** 2015. Stochastic electrotransport selectively enhances the transport of highly electromobile molecules. Proc. Natl. Acad. Sci. USA *112*:E6274-E6283.
20. **Zukor, K.A., D.T. Kent, and S.J. Odelberg.** 2010. Fluorescent whole-mount method for visualizing 3-dimensional relationships in intact and regenerating adult newt spinal cords. Dev. Dyn. *239*:3048-3057.

Received 14 July 2016; accepted 04 January 2017.

Address correspondence to: Jian-Guo Qi, MD, PhD, Department of Histology, Embryology and Neurobiology, West China School of Preclinical and Forensic Medicine, Sichuan University, No 17, Section 3, South Ren-Min Road, Chengdu, Sichuan,610041, China. E-mail: jgqi@scu.edu.cn